3D Geological Modeling Method for Normal Pressure Shale Gas

Jiangyou Chen, Zongyun Chen*, Zhiliang Zhao, Liping Cao and Hong Yu

Guizhou Shale Gas Exploration and Development Co., Ltd. Zhunyi, China

*42346385@qq.com

Abstract. 3D geological modeling technique, as a comprehensive characterization method for oil and gas reservoirs, is widely applied in the process of oil and gas field development. Addressing the challenge of unclear geological characteristics in the early exploration stage of atmospheric shale gas reservoirs, this study employs a modeling workflow encompassing structural modeling, stress field modeling, fracture modeling, lithofacies modeling, attribute modeling, porosity modeling, permeability modeling, total organic carbon content modeling, and gas content modeling. The established models successfully predict the geological features of the reservoir in the study area. This model can provide support for well deployment, drilling tracking, and hydraulic fracturing design.

Keywords: Energy security, Guizhou shale gas, Normal pressure reservoir, 3D geological modeling, Shale gas development.

1 Introduction

Three-dimensional geological modeling refers to the integration of seismic, geological, well logging, well testing, and reservoir engineering data through computer-aided methods [1-3] to comprehensively and quantitatively characterize structural features, sedimentary facies distribution, and reservoir attributes [4-7]. This technology is widely employed in the development process of oil and gas fields [8-11], particularly serving as a crucial technique in the integrated development of shale gas geological engineering [12-16].

The Fu Yan Block is located in Guizhou Province, characterized by typical karst topography. The terrain in the work area is generally higher in the northwest and lower in the southeast, with elevations ranging between 600 and 1429 meters. Undergoing multiple tectonic movements since the Late Paleozoic, subjected to strong compressional stress from the southeast, the Fu Yan Block exhibits the structural characteristics of a narrow, northeast-trending thrust-fold belt. During the Late Ordovician Five Fingers Formation sedimentation period, the study area formed a stable set of organic-rich mud shale, overlain by biotic mud limestone at the top of the Five Fingers Formation. In the early Silurian period, the Fu Yan Block was in a relatively

A. E. Abomohra et al. (eds.), *Proceedings of the 2023 9th International Conference on Advances in Energy Resources and Environment Engineering (ICAESEE 2023)*, Atlantis Highlights in Engineering 29,
https://doi.org/10.2991/978-94-6463-415-0_22

quiet, low-energy, and strongly reducing deep-water continental shelf environment. The Longmaxi Formation deposited a set of black carbonaceous mud shale with enrichments of pyrite and organic matter. The vitrinite reflectance in the study area ranges from 1.92% to 2.19%, with an average of 2.06%. The kerogen is in the high maturity to over-maturity evolution stage, with the targeted Five Fingers Formation-Longmaxi Formation shale having a total organic carbon content ranging from 0.24% to 5.79%, with an average of 4.05%. Regarding reservoir characteristics, the predominant pore types are organic pores and dissolution pores, with minimal microfractures and intercrystalline pores. Core analysis test results indicate a porosity range of 3.25% to 4.85%, with an average of approximately 4.1%. The permeability varies from 0.0003 to 0.0804 mD, with an average of 0.011 mD. In terms of gas content, on-site analysis of Well 1 in Fu Di reveals a total gas content ranging from 3.04 to 5.68 m3/t, with an average of about 4.39 m3/t. For Well 1 in Fu Ye, the analyzed gas content ranges from 0.8 to 1.66 m3/t, with an average of 1.2 m3/t, and the total gas content ranges from 2.3 to 5.6 m3/t, with an average of approximately 3.5 m3/t. Overall, the gas content is relatively good.

2 Materials and methods

The data utilized in the modeling process include well coordinates, core elevation, well trajectory, and other well-related data, geological layering data, single-well lithofacies data, logging curves, logging interpretation results, and seismic data such as three layers of depth-domain seismic interpretation, depth-domain acoustic impedance, amplitude volumes, and depth-domain fracture prediction ant bodies.

Traditional modeling approaches typically follow a workflow involving structural modeling, lithofacies determination, reservoir property characterization, and fracture modeling [17-20]. In this study, based on the fundamental characteristics of atmospheric shale gas reservoirs, a novel modeling approach was developed by integrating geological, seismic, well logging, and core analysis data. Analysis of single-well stratigraphic division results, structural interpretation results, detailed logging interpretation results, and precise characterization of physical properties informed the innovative creation of structural models, stress field models, fracture models, and lithofacies models. Under the control of the lithofacies model, attribute models for porosity, permeability, total organic carbon content, gas content, and others were established.

3 Results

In accordance with the geological features of the Fu Yan Block, the modeling work area is strategically oriented at 55° to align with the elongation of the anticline. Encompassing a substantial 102 square kilometers, the planar grid resolution is meticulously set at 20×20 meters. The targeted layer, ranging from 5 to 20 meters, is intricately partitioned into 40 layers, each approximately 0.4 meters thick. The comprehensive modeling comprises a total of 1,198,000 grids, meticulously configured to meet the stringent accuracy criteria of the model.

3.1 A Subsection Sample

Drawing upon the outcomes of structural interpretation, a comprehensive set of 81 fault models has been meticulously crafted for the study area. Predominantly oriented in the northeast, these faults exhibit lengths ranging from 199 to 3595 meters and throws varying from 15 to 583 meters (Figure.1). Leveraging well-point geological layering data as the cornerstone and employing depth-domain structural planes as trend surfaces, a rigorous alignment between well-point layering data and structural planes is ensured. This meticulous process results in the creation of a three-dimensional structural model characterized by authenticity, logical coherence, and adherence to precision standards. Notably, six planes — O_3w, O_3g, $S_1l_1^1$, $S_1l_1^2$, $S_1l_1^3$, $S_1l_1^4$—have been established, as depicted in Figure 2. The structural and stratigraphic models not only align with structural trends but also incorporate real drilling insights, with grid volumes for stratigraphic units meticulously ranging from 0 to 1197 cubic meters, and the absence of negative volume grids.

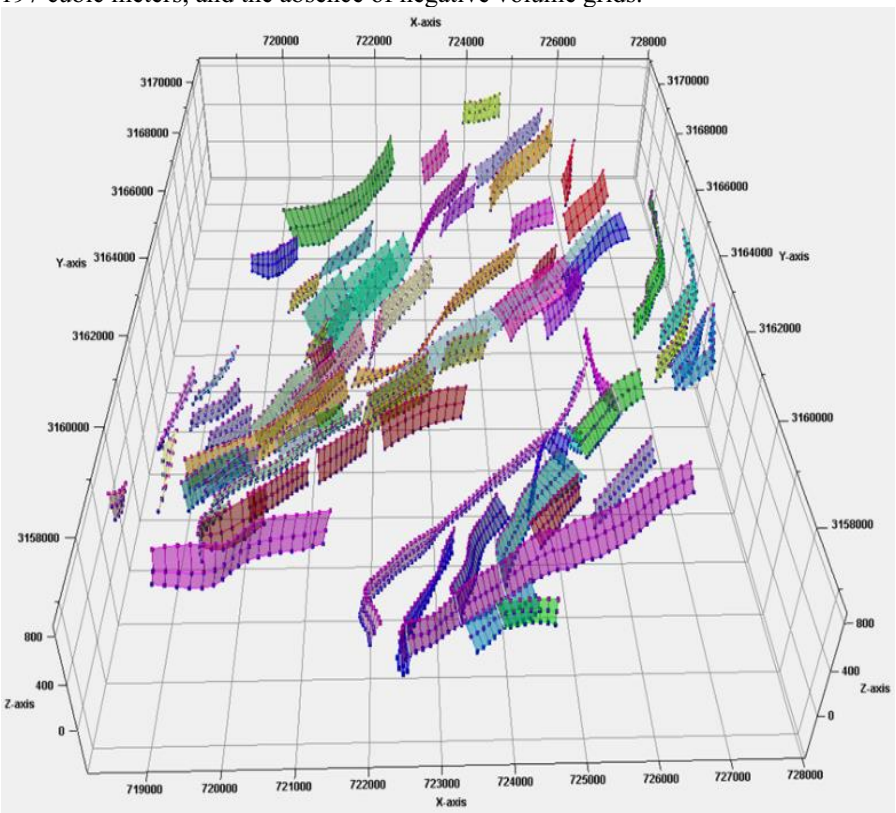

Fig. 1. 3D fault model of Fuyan Block.

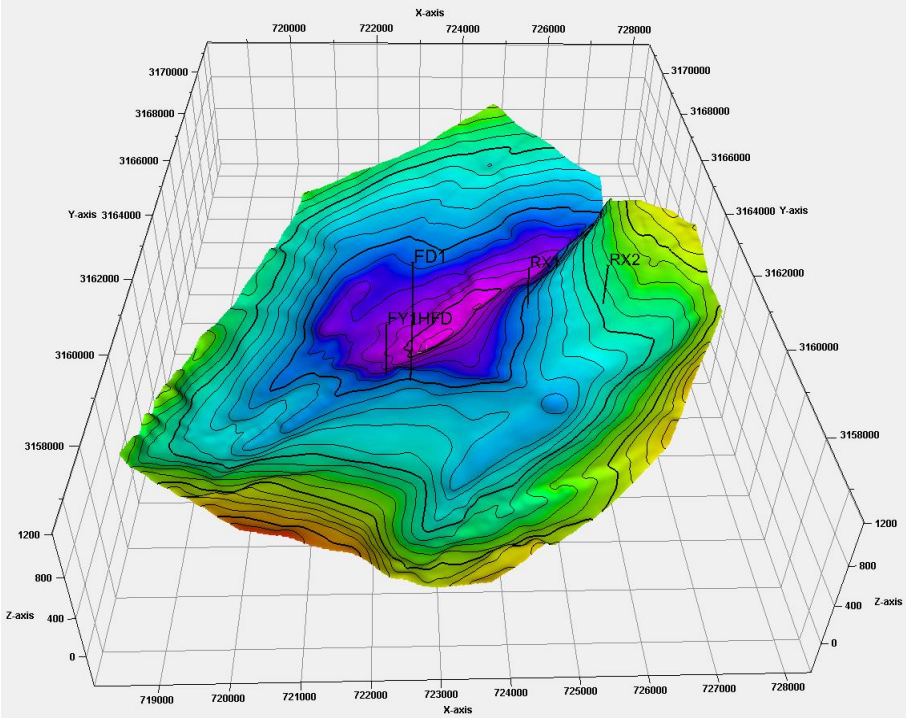

Fig. 2. 3D surface model of Fuyan Block

3.2 Geostress Model

The spatial distribution of geostress within the Longmaxi Formation of the Fu Yan Block is intricately shaped by the compounding effects of overlying strata pressure and burial depth. Leveraging parameters encompassing the average density of upper formations, topography maps, stress gradients, as well as geophysically-derived data on Young's modulus and Poisson's ratio, coupled with insights into the regional principal stress direction, a meticulous geostress stress model has been devised for the block. This model prognosticates the nuanced distribution of stress within the target layer. The resulting model portrays overlying strata pressure ranging from approximately 2.0 to 16.0 MPa. Notably, areas with thinner overlying strata, particularly in the eastern and southern sectors of the inclined block, exhibit lower overlying strata pressure. Conversely, regions characterized by thicker overlying strata, primarily in the core and western expanses, correspond to higher overlying strata pressure. Within the Longmaxi Formation of the Fu Yan Block, the maximum principal stress is estimated to range from 2.5 to 27.5 MPa. Notably, the eastern wing of the Fu Yan anticline registers lower maximum principal stress values, while the western wing experiences comparatively higher values. Stress concentration is particularly conspicuous in the core region, aligning with areas of pronounced structural deformation and active fault development, where the geostress is notably elevated (Figure. 3).

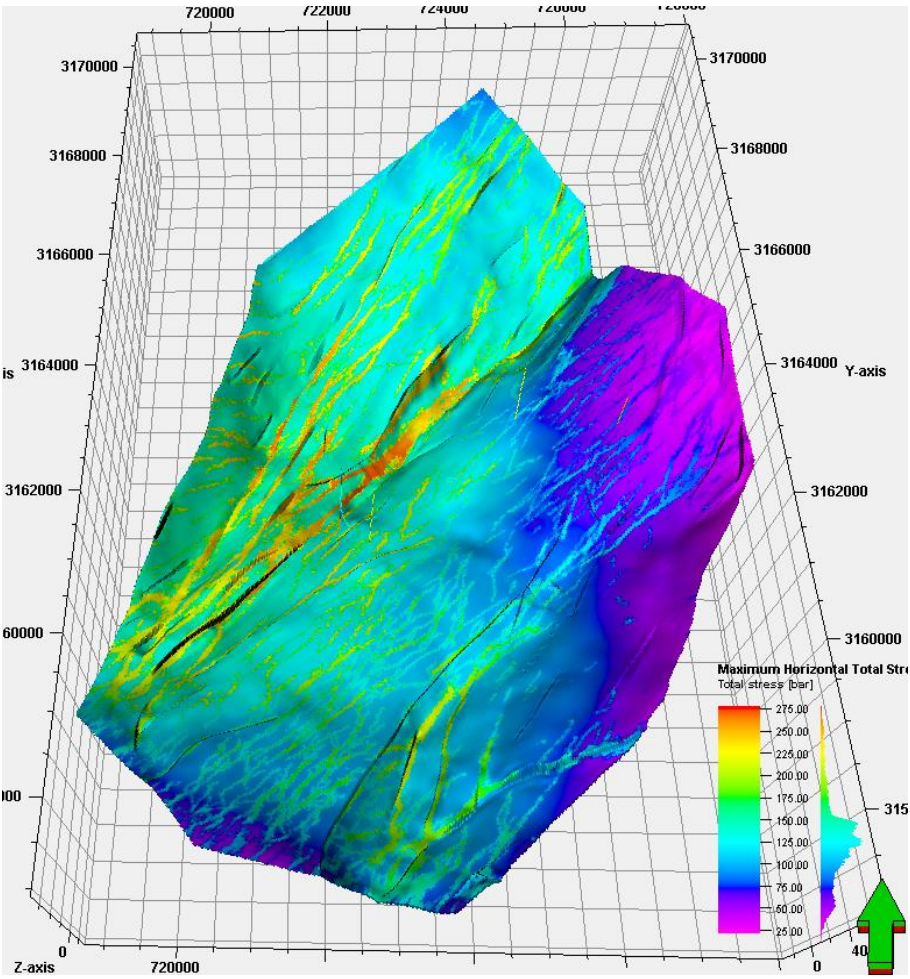

Fig. 3. Geostress model of Fuyan Block

3.3 Fracture Model

Building upon the established geostress stress framework, this modeling initiative relies significantly on ant body recognition technology applied to post-stack seismic data for the anticipation of natural fractures. The "Ant Tracking Algorithm," an intricate seismic attribute algorithm developed by Schlumberger, has been harnessed for its suitability in modeling large-scale fractures. A novel facet, the "Vector Ant Tracking Technology," has been introduced, involving the systematic tracking of ant bodies in diverse directions based on the principal orientation of fault systems and large-scale fractures. This process facilitates the extraction of significant fracture segments. The fundamental principle at play entails the dissemination of a multitude of virtual ants across seismic data. Ants that meet predefined conditions release pheromones,

attracting other ants to trace fracture locations. The application of this technology, synergized with profile fracture interpretation and attribute map fracture distribution, facilitates the spatial tracking of fractures. Notably, the core region of the anticline emerges as a zone characterized by concentrated geostress stress, fostering well-developed fractures, primarily oriented in a northeast direction (Figure.4).

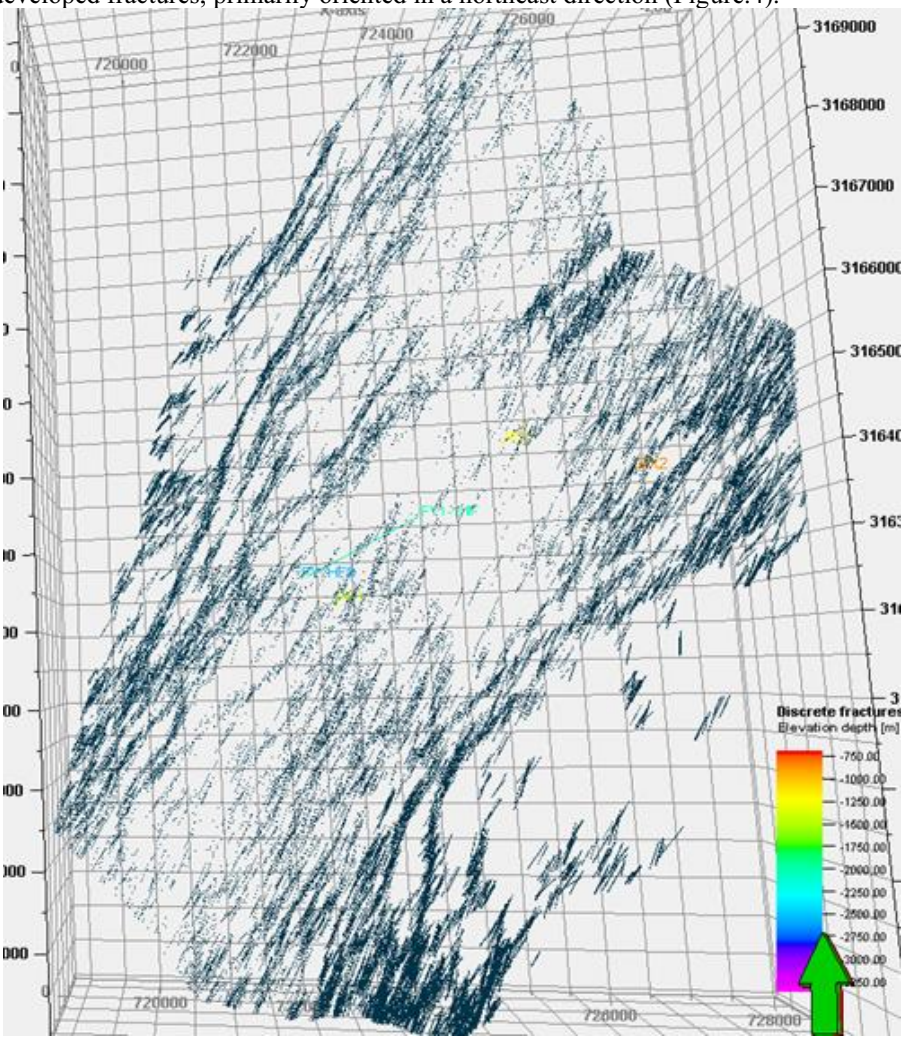

Fig. 4. Fracture model of Fuyan Block

3.4 Facies Model

Initiating the process, lithology data from well log interpretations is discretized and incorporated into a grid model. Subsequently, a comprehensive data analysis is conducted, focusing on the vertical distribution and variogram functions associated with

lithofacies. Guided by the distinctive characteristics of regional sedimentary facies distribution and integrating insights from lithofacies distribution in individual wells, a methodical approach using sequential indicator simulation is adopted. The objective is to craft a lithofacies model specific to shale reservoirs, effectively capturing the spatial distribution nuances of carbonaceous mudstone, carbonaceous shale, and interbedded limestone (Figure.5).

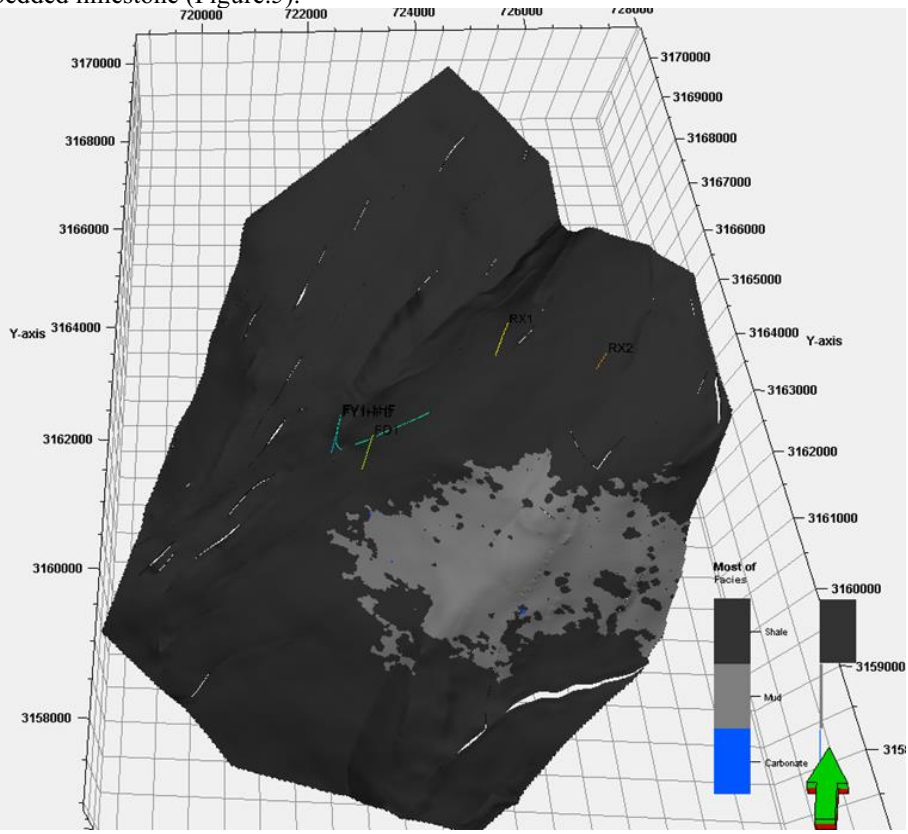

Fig. 5. Facies model of Fuyan Block

3.5 Petrophysical Model

Based on well logging interpreted petrophysical data and under the control of a three-dimensional lithofacies model, a three-dimensional attribute model is established using sequential Gaussian simulation, with seismic fracture data and petrophysical statistical analysis results serving as constraints (Figure.6). The simulated porosity results align closely with the observed porosity distribution patterns, ranging from 1.3% to 5.4%, with a main value range of 4.5% to 5.4% and an average of 4.4%. On a planar scale, there is relatively little variation in porosity across the study area, with higher porosity values in the core region of the anticline. Vertically, porosity gradually decreases with increasing burial depth, and the $S_1l_1^3$ layer exhibits relatively higher

porosity. The simulated permeability results closely mirror the observed permeability distribution patterns, ranging from 0.012 to 0.045 mD, with a main value range of 0.035 to 0.045 mD and an average of 0.034 mD. On a planar scale, the core region and southern part of the anticline exhibit relatively higher permeability values. Vertically, the $S_1l_1^3$ layer shows relatively higher permeability. Results for total organic carbon content closely correspond to the observed distribution patterns, ranging from 0.01% to 5.72%, with a main value range of 3% to 5% and an average of 3.69%. On a planar scale, the central part of the block exhibits relatively higher total organic carbon content. Vertically, the $S_1l_1^1$ layer shows relatively higher total organic carbon content. The simulated gas content results closely align with the observed distribution patterns, ranging from 2.1% to 5.25%, with a main value range of 3.8% to 4.4% and an average of 3.88%. On a planar scale, the central part of the block exhibits relatively higher gas content, and vertically, the $S_1l_1^1$ layer shows relatively higher gas content.

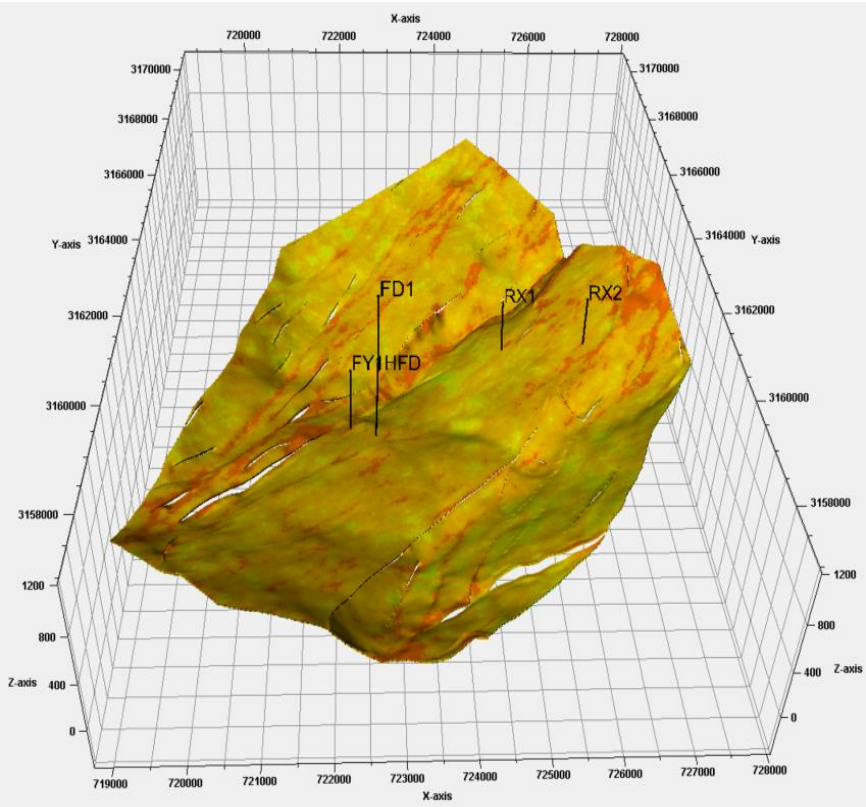

a) 3D porosity model

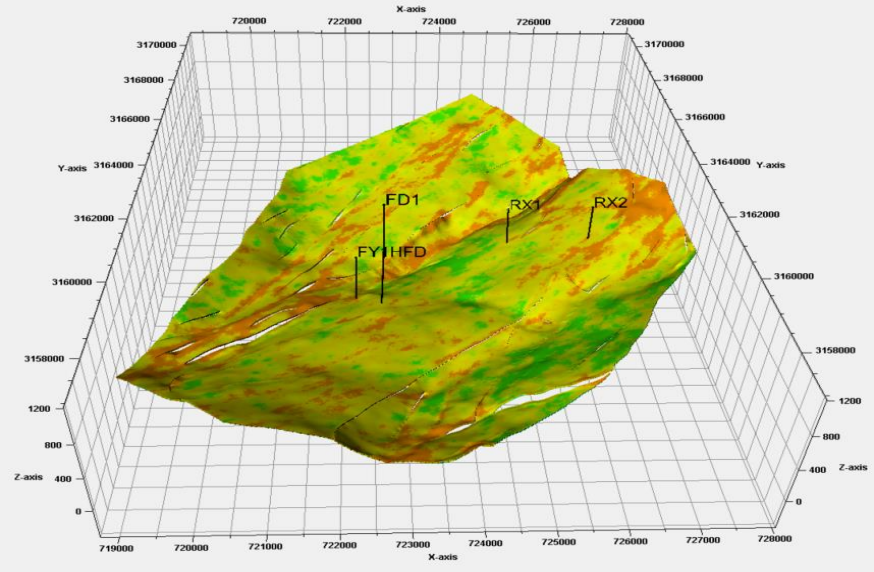

b) 3D permeability model

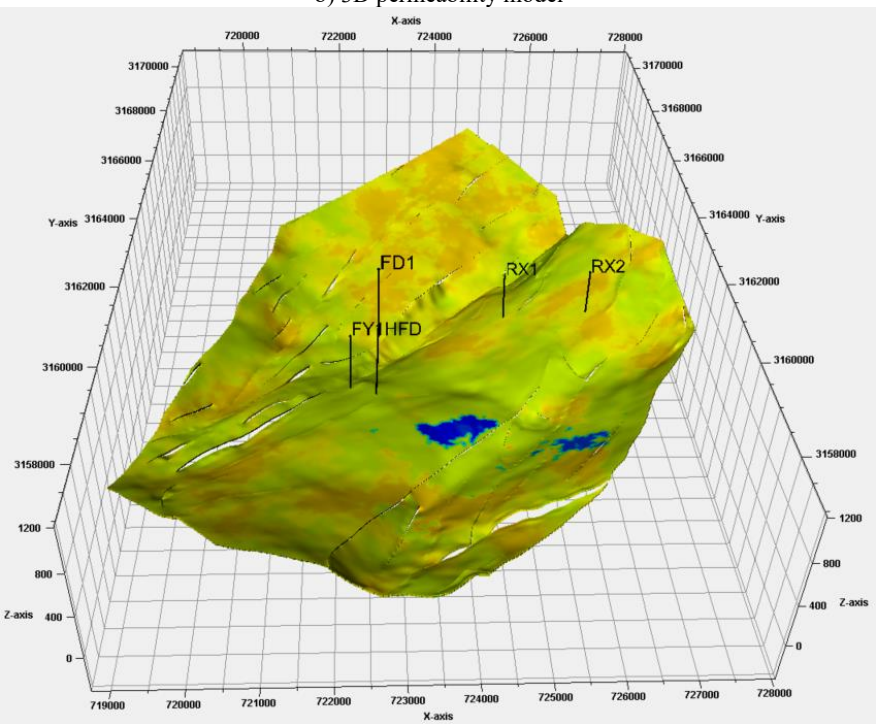

c) 3D TOC model

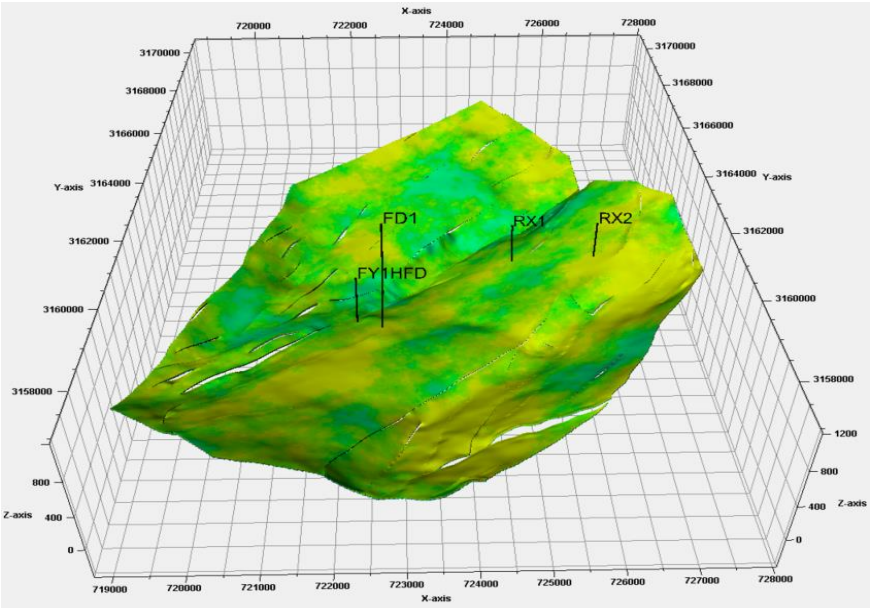

d) 3D gas saturation model

Fig. 6. 3D petrophysical model of Fuyan Block

3.6 Model Application

Based on the results of structural characterization, the 3D structural model is used to accurately characterize the structure and surface distribution. Based on the fault distribution and the surface of structural model, the drilling of FY-1HF well is improved significantly by guiding geological guidance tracking while drilling. In the geological model, the facies, porosity, permeability, TOC and gas content of the target zone are in basically consistent with the well logging (Figure 7).

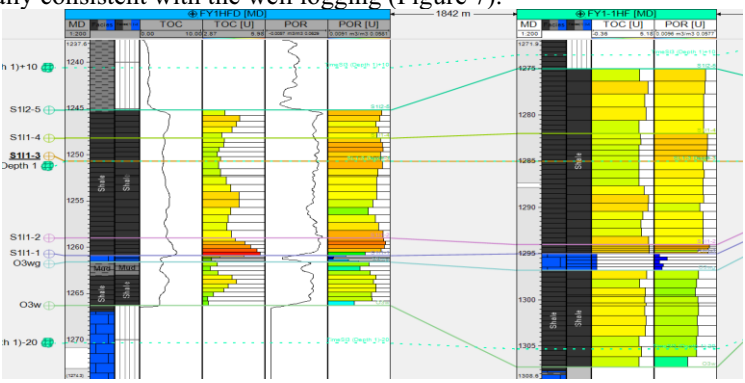

Fig. 7. Model verification of Fuyan Block

4 Discussion

Integrated seismic fracture characterization and stratigraphic tracking results are used to refine the three-dimensional structural model, providing detailed insights into the structural and stratigraphic distribution within the block. Guided by the distribution of faults and the deformations observed in the structural model, geological steering while drilling is implemented, significantly enhancing the drilling encounter rate of reservoirs in wellbore trajectory of the Fu Yan 1HF well. Utilizing the comprehensive seismic fracture prediction volume, the three-dimensional fracture model is employed to finely represent the spatial distribution characteristics of fractures within the block. Combining information on in-situ stress and fracture distribution characteristics, this approach can guide the deployment of horizontal well locations and the design of engineering schemes in the Fu Yan Block. Built upon single-well data, the three-dimensional attribute model is applied to finely characterize the heterogeneity features of the reservoir. The geological model includes lithofacies, porosity, permeability, total organic carbon content, and gas content within the target reservoir interval. The simulation results closely match the well data, providing a strong foundation for subsequent reservoir evaluation and the formulation of development strategies.

5 Conclusion

The Fu Yan Block exhibits a narrow and elongated northeast-trending anticline, with the target reservoir interval consisting of black shale from the Five Member Formation to the Longmaxi Formation. This geological formation presents favorable conditions for hydrocarbon generation, characterized by well-developed organic pores, high gas content, and good compressibility. On a planar scale, the core region of the anticline displays relatively higher porosity and permeability values, while the central part of the Fu Yan Block exhibits higher total organic carbon content and gas content. Vertically, the $S_1l_1^3$ and $S_1l_1^1$ layers exhibit relatively higher porosity and permeability values, while the $S_1l_1^1$ and $S_1l_1^4$ layers show higher total organic carbon content and gas content. In response to the geological characteristics of the atmospheric-pressure shale gas reservoir, an innovative modeling workflow is introduced, encompassing the construction of a structural-stress-fracture-lithofacies-attribute model. This model aligns closely with the initial geological understanding, demonstrating a high degree of compatibility with well data and overall credibility. The application of this model to guide geological steering while drilling significantly enhances the encounter rate of reservoirs during actual drilling, providing substantial support for reservoir evaluation and the formulation of development strategies.

References

1. Jia A, Guo J, He D (2007) Perspective of Development in Detailed Reservoir Description. Petroleum Exploration and Development 34:691–695. https://doi.org/10.3321/j.issn:1000-0747.2007.06.010.
2. Wu S, Li Y (2007) Reservoir Modeling: Current Situation and Development Prospect. Marine Origin Petroleum Geology 12:53–60. https:// doi.org/ 10.3969/ j.issn. 1672-9854. 2007.03.009.
3. Li Q, Zhang L, Cao D, et al (2016) Usage, Status, Problems, Trends and Suggestions of 3D Geological Modeling. Geology and Prospecting 52:759–767. https:// doi. org/ 10. 13712/j.cnki.dzykt.2016.04.018.
4. Ursegov SO, Zakharian AZ, Serkova VI (2021) Adaptive Geological Modelling and Its Application for Petroleum Reservoir Conditions. Earth science 666:1–7. https: // doi. org/ 10.1088/1755-1315/666/2/022065.
5. Laudadio AB, Schetselaar EM, Mungall JE, Houlé MG (2022) 3D Modeling of the Esker Intrusive Complex, Ring of Fire Intrusive Suite, Mcfaulds Lake Greenstone Belt, Superior Province: Implications for Mineral Exploration. Ore Geology Reviews 145:1–23. https: // doi.org/10.1016/j.oregeorev.2022.104886.
6. Berrone S, Raeli A (2022) Efficient Partitioning of Conforming Virtual Element Discretizations for Large Scale Discrete Fracture Network Flow Parallel Solvers. Engineering Geology 306:1–16. https://doi.org/10.1016/j.enggeo.2022.106747.
7. Shi C, Wang Y (2022) Data-driven Construction of Three-dimensional Subsurface Geological Models from Limited Site-specific Boreholes and Prior Geological Knowledge for Underground Digital Twin. Tunnelling and Underground Space Technology 126:1–16. https://doi.org/10.1016/j.tust.2022.104493.
8. Yan L, Liu Q, Liu X (2022) Research on 3D Geological Modeling of Fractured-vuggy Carbonate Reservoirs. Energy Reports 8:491–500. https: //doi. org/ 10. 1016 /j. egyr. 2022. 03.052.
9. Lopes JAG, Medeiros WE, La Bruna V, et al (2022) Advancements Towards DFKN Modelling: Incorporating Fracture Enlargement Resulting from Karstic Dissolution in Discrete Fracture Networks. Journal of Petroleum Science and Engineering 209:1–18. https: // doi. org/10.1016/j.petrol.2021.109944.
10. Liu Z, Zhang Y, Zhang Y, et al (2022) Influencing Factor Analysis on the Fractured Tight Sandstone Gas Reservoir Characteristics: A Case Study of Bozi 3 Gas Reservoir in the Tarim Basin. Frontiers in Earth Science 10. https://doi.org/10.3389/feart.2022.881934.
11. Ferrer R, Emery X, Maleki M, Navarro F (2021) Modeling the Uncertainty in the Layout of Geological Units by Implicit Boundary Simulation Accounting for a Preexisting Interpretive Geological Model. Nat Resour Res 30:4123–4145. https://doi.org/10.1007/s11053-021-09964-9.
12. Lyu M, Ren B, Wu B, et al (2021) A Parametric 3D Geological Modeling Method Considering Stratigraphic Interface Topology Optimization and Coding Expert Knowledge. Engineering Geology 293:1–17. https://doi.org/10.1016/j.enggeo.2021.106300.
13. Hillier M, Wellmann F, Brodaric B, et al (2021) Three-Dimensional Structural Geological Modeling Using Graph Neural Networks. Math Geosci 53:1725–1749. https: // doi. org/ 10.1007/s11004-021-09945-x.
14. Ceccato A, Viola G, Antonellini M, et al (2021) Constraints Upon Fault Zone Properties by Combined Structural Analysis of Virtual Outcrop Models and Discrete Fracture Network Modelling. Journal of Structural Geology 152:1–18. https: // doi. org/ 10. 1016/ j.jsg.2021.104444.

15. Bolós X, Oms O, Rodríguez-Salgado P, et al (2021) Eruptive Evolution and 3D Geological Modeling of Camp Dels Ninots Maar-diatreme (Catalonia) Through Continuous Intra-crater Drill Coring. Journal of Volcanology and Geothermal Research 419:1–10. https://doi.org/10.1016/j.jvolgeores.2021.107369.
16. Azim RA (2021) Estimation of Fracture Network Properties from FMI and Conventional Well Logs Data Using Artificial Neural Network. Upstream Oil and Gas Technology 7:1–16. https://doi.org/10.1016/j.upstre.2021.100044.
17. Almedallah MK, Al Mudhafar AA, Clark S, Walsh SDC (2021) Vector-based Three-dimensional (3D) Well-path Optimization Assisted by Geological Modelling and Bore-hole-log Extraction. Upstream Oil and Gas Technology 7:1–14. https: // doi. org/ 10. 1016/ j.upstre.2021.100053.
18. Liu Z, Zhang Y, Liu H, et al (2021). Fine Scale Geological Modeling Techniques in Kela 2 Gas Field. Journal of Petroleum & Environmental Biotechnology. 12:1-6.
19. Liu Z, Chen D, Gao Z, et al (2023) 3D geological modeling of deep fractured low porosity sandstone gas reservoir in the Kuqa Depression, Tarim Basin. Frontiers in Earth Science.
20. Krajnovich A, Zhou W, Gutierrez M (2020) Uncertainty Assessment for 3D Geologic Modeling of Fault Zones Based on Geologic Inputs and Prior Knowledge. Solid Earth 11:1457–1474. https://doi.org/10.5194/se-11-1457-2020.